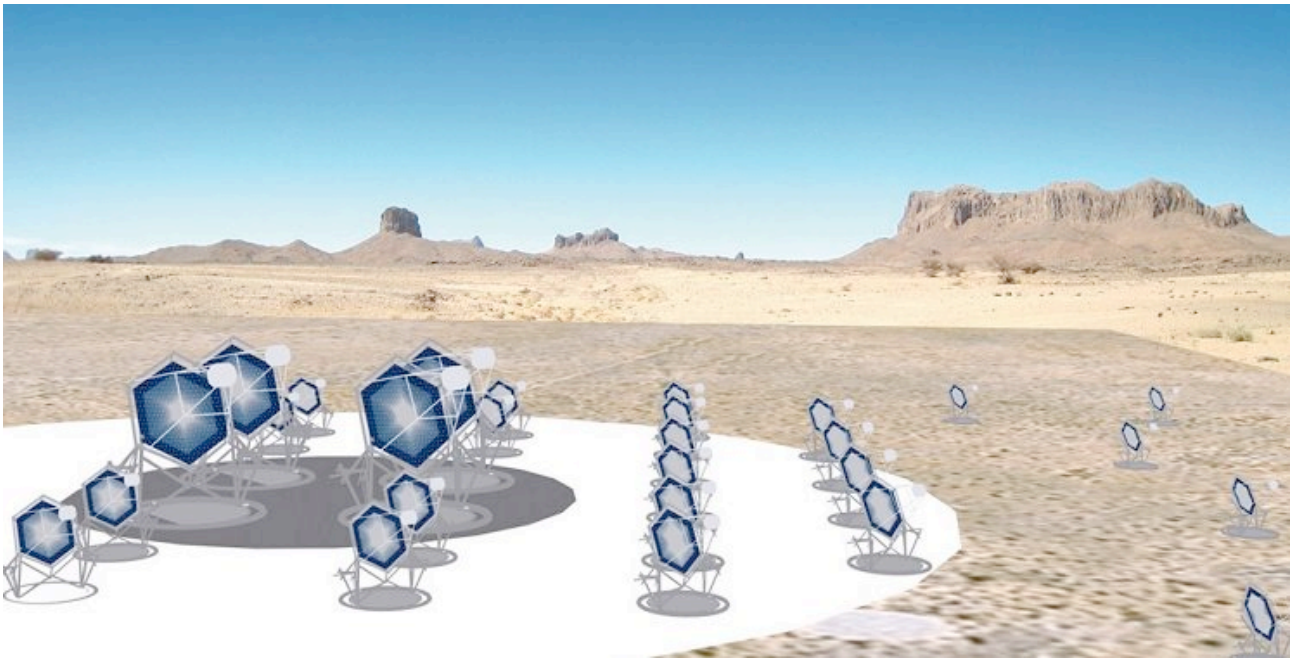
Error Budget Tree for the ASTRI prototype: structure and mirrors



Prepared by: Name: Rodolfo Canestrari
Paolo Conconi
Enrico Giro
Gabriele Rodeghiero
Signature:
Date: 14/01/2014

All information contained in this document is property of **INAF.** All rights reserved.

TABLE OF CONTENTS

DISTRIBUTION LIST **3**

DOCUMENT HISTORY **4**

LIST OF ACRONYMS **5**

APPLICABLE DOCUMENTS **5**

REFERENCE DOCUMENTS **5**

1. INTRODUCTION **6**

2. DEFINITIONS **7**

2.1 Reference system 7

2.2 Sensitivity 8

3. ERROR BUDGET TREE RELATED TO M1 ..... **9**

4. ERROR BUDGET TREE RELATED TO M2 ..... **11**

4.1 Profile errors 11

4.2 Alignment errors 11

5. ERROR BUDGET TREE RELATED TO CAM **13**

5.1 Profile errors 13

5.2 Alignment errors 13

5.3 PDMs tolerances 13

5.4 PMMA window tolerances 13

6. TOLERANCE STUDY ON ERROR BUDGET **15**

6.1 RMS Radius modifications 15

6.2 Centroid shift estimations 19

All information contained in this document is property of **INAF.** All rights reserved.

DISTRIBUTION LIST

ASTRI ML	astri@brera.inaf.it

All information contained in this document is property of **INAF.** All rights reserved.

DOCUMENT HISTORY

Version	Date	Modification
1	04/11/2011	first version
2	02/04/2012	Add chapter on Camera
3	14/01/2014	Add chapter on PDMs tolerance New chapter on Tolerance study

All information contained in this document is property of **INAF.** All rights reserved.

LIST OF ACRONYMS

CAM	Camera, Cherenkov detector
FoV	Field of View
M1	Primary Mirror
M2	Secondary Mirror
PDM	Photo Detection Module
PMMA	Polymethyl methacrylate
PSF	Point Spread Function
PV	Peak to Valley
R80	Radius containing the 80% of the PSF
RMS	Root Mean Square

APPLICABLE DOCUMENTS

[AD1]

REFERENCE DOCUMENTS

[RD1] ASTRI-IR-OAB-3100-009 *"The optical layout of the ASTRI prototype: 4 meter Schwarzschild-Couder Cherenkov telescope for CTA with 10° of field of view"*

[RD2]

All information contained in this document is property of **INAF.** All rights reserved.

1. INTRODUCTION

This document describes the Error Budget Tree to be used for the design and verification of the structure and mirrors subsystems of the ASTRI telescope prototype.

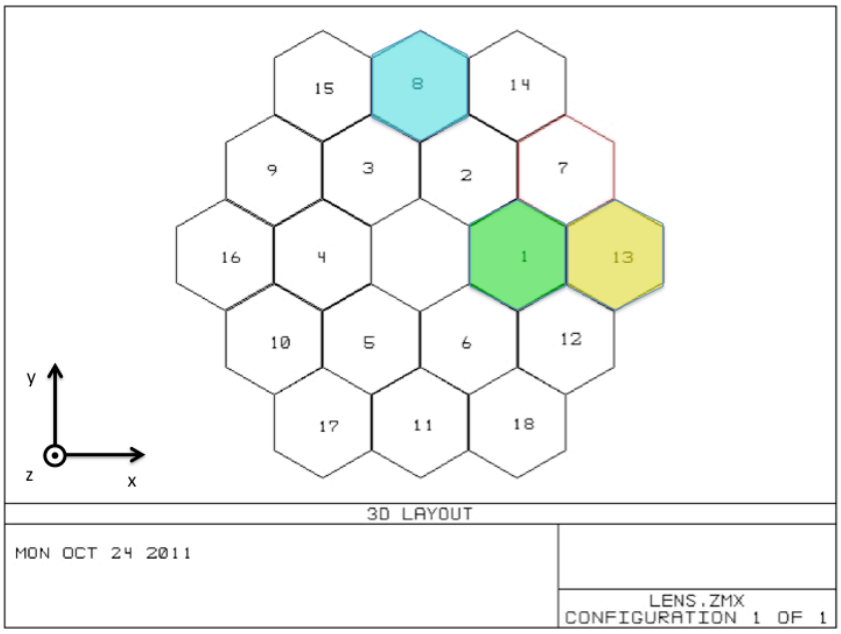
This document is a living document. This means that the numbers adopted for each parameter can be subject of changes depending from the outcomes of the structural analyses and/or technological developments.

All information contained in this document is property of **INAF.** All rights reserved.

2. DEFINITIONS

2.1 Reference system

The reference system is defined as in figure, if not explicitly stated. The *z* axis is the optical axis and it points toward the M2.



According to the M1 segments numeration, we give the nominal position of the centers of each hexagon. The numbers are in mm unit.

N° dell'esagono	X	Y	Z
1	856.485	0.0	44.229
2	428.242	741.378	44.229
3	-428.242	741.378	44.229
4	-856.485	0	44.229
5	-428.242	-741.378	44.229
6	428.242	-741.378	44.229
7	1280.522	738.775	129.652
8	0.0	1478.620	129.652
9	-1280.522	739.310	129.652
10	-1280.522	-739.319	129.652
11	0.0	-1478.620	129.652
12	1280.522	-739.310	129.652
13	1704.850	0.0	170.581
14	852.425	1476.443	170.581
15	-852.425	1476.443	170.581
16	-1704.850	0.0	170.581
17	-852.425	-1476.443	170.581
18	852.425	-1476.443	170.581

The segments numbered 1, 8 and 13 are used as reference and they correspond to the color index green, light blue and yellow respectively.

All information contained in this document is property of **INAF.** All rights reserved.

2.2 Sensitivity

As described in [RD1] the optical layout of the ASTRI prototype has the energy concentration (ensquared energy) greater then 80% into the Cherenkov pixels along the entire field of view.

This definition is meaningful taking into account the entire telescope optical design and is not referred to the single mirror segments, like in the Davies-Cotton case. Considering this fact the Error Budget Tree hereafter described can be compiled in such a way the global effect of all contributions keeps the energy concentration (ensquared energy) better then (or equal to) 70%.

This can be translated in a PV error budget equal to 120 μm and slope error budget equal to 60'' rms.

All information contained in this document is property of **INAF.** All rights reserved.

3. ERROR BUDGET TREE RELATED TO M1

Let's consider the secondary mirror M2 being monolithic, infinitely rigid and having the nominal profile.

			Value		Units	Comments
1. M1 segments profile errors						
	1.1. Manufacturing					
		a. Mold	30 10	-- --	µm PV " rms	It comes from FLABEG, no/very poor control on it. The rms is sampled at least with a grid of 25 mm of pitch.
		b. Replication process	50 10	-- --	µm PV " rms	It comes from FLABEG, limited control on it. The rms is sampled at least with a grid of 25 mm of pitch.
		c. Glass cutting	--	6	'	Axial (normal to the surface on the hexagon center) rotation of the glass profile wrt the nominal one. It is equivalent to 0.87 mm over the length of the hexagonal side.
		d. Integration	TBD TBD	-- --	µm PV " rms	Contribution of the cold shaping step (could be also improvements)
		SUBTOTAL	***58*** ***--***	***--*** ***6***	***µm PV*** ***'***	***Quadratic propagation***
	1.2. Structural					
		a. Mounting	40 2		µm PV " rms	Contribution of the mounting supports (e.g. gluing of the interfaces, …) The shape will be modified only locally.
		b. Gravity	30 TBC		µm PV " rms	Contribution of the normal gravity
		c. Operative wind	30 TBC		µm PV " rms	Contribution of the operative wind
		d. Operative temp.	1		µm PV	Homogeneous temperature shift up to ±20°C
		SUB TOTAL	***58***		***µm PV***	***Quadratic propagation***
	GRAND TOTAL		***82***		***µm PV***	***Error budget in quadratic propagation.***
2. M1 segments alignment errors						
	2.1 Translations					
		a. x	±2		mm	These values are referred to the positions of the centers of the hexagons as reported in Table 1.
		b. y	±2		mm	
		c. z	±4		mm	

All information contained in this document is property of **INAF.** All rights reserved.

	2.2 Rotations				
		a. z'	±4	'	*z'* is defined as the axis parallel to the *z* (optical axis) passing through the center of the hexagons.
	2.3 Tilts				
		a. x	±30	''	
		b. y	±30	''	

Not appreciable degradation (i.e. <5%) of the ensquared energy is reported within these values. There is no need to actively correct with actuators within these ranges. However, these values shall be used to define the accuracy and the range of the actuators.

All information contained in this document is property of **INAF.** All rights reserved.

4. ERROR BUDGET TREE RELATED TO M2

4.1 Profile errors

Let's consider now the M1 segments being perfectly aligned, infinitely rigid (both the mirrors themselves and the telescope structure) and having the nominal profile.

We consider now the contributions coming from a not perfect secondary mirror.

4.2 Alignment errors

The positioning errors along (*x, y*) and the relative tilts translate almost completely in pointing errors of the telescope (the contribution to the ensquared energy is negligible).

The error along *z* is a defocusing of the telescope and can be correct adjusting the 3 actuators of M2.

			Value	Units	Comments
3. M2 profile errors					
	3.1. Manufacturing				
		a. Mold	120 40	µm PV '' rms	It comes from FLABEG, no/very poor control on it. The rms is sampled at least with a grid of 25 mm of pitch.
		b. Replication process	200 40	µm PV '' rms	It comes from FLABEG, limited control on it. The rms is sampled at least with a grid of 25 mm of pitch.
		c. Glass cutting	n.a.	'	Axial (normal to the surface on the hexagon center) rotation of the glass profile wrt the nominal one.
		d. Integration	TBD TBD	µm PV '' rms	Contribution of the cold shaping step (could be also improvements)
		SUBTOTAL	***217*** ***(54)***	***µm PV*** ***µm PV***	***Quadratic propagation*** ***(calculated taking into account the demagnification factor, equal to 4)***
	3.2. Structural				
		a. Mounting	40 2	µm PV '' rms	Contribution of the mounting supports (e.g. gluing of the interfaces, …) The shape will be modified only locally.
		b. Gravity	120 TBC	µm PV '' rms	Contribution of the normal gravity
		c. Operative wind	120 TBC	µm PV '' rms	Contribution of the operative wind
		d. Operative temp.	4	µm PV	Homogeneous temperature shift up to ±20°C
		SUBTOTAL	***174*** ***(44)***	***µm PV***	***Quadratic propagation*** ***(calculated taking into account the***

All information contained in this document is property of **INAF.** All rights reserved.

				µm PV	***demagnification factor, equal to 4)***
	GRAND TOTAL		***278***	***µm PV***	***Error budget in quadratic propagation.***
			(69)	***µm PV***	***(calculated taking into account the demagnification factor, equal to 4)***
4. M2 alignment errors					
	4.1 Translations				
		a. x	±3	mm	This introduces pointing errors to be modeled with T-point. (1 mm = 38'' pointing error)
		b. y	±3	mm	
		c. z	±4	mm	Relative to M1
			±1	mm	Relative to CAM
	4.2 Rotations				
		a. z	n.a.	‘	
	4.3 Tilts				
		a. x	10	‘	The tilts do not constrain the design of the telescope structure up to the indicated value. Obliviously, this introduces pointing errors to be modeled with T-point.
		b. y	10	‘	

All information contained in this document is property of **INAF.** All rights reserved.

5. ERROR BUDGET TREE RELATED TO CAM

5.1 Profile errors

Let's consider now the M1 segments and M2 monolithic mirror perfectly aligned, infinitely rigid (both the mirrors themselves and the telescope structure) and having the nominal profile.

We consider now the contributions coming from a not perfect camera mounting.

5.2 Alignment errors

The positioning errors along (*x, y*) translate almost completely in pointing errors of the telescope (the contribution to the ensquared energy is negligible). Nevertheless, we fix the maximum displacements to ±5.5 mm along each axis (*x, y*).

Tilts errors along (*x, y*) of the order of 20 arcmin for each axes can be tolerable.

The error along *z* is a defocusing of the telescope and is correct adjusting the 3 actuators of M2.

5.3 PDMs tolerances

5. PDM alignment errors					
	5.1 Translations				
		a. x	±1	mm	Relative to focal plane mechanical structure
		b. y	±1	mm	
		c. z	±1	mm	
	5.2 Rotations				
		a. z	n.a.	‘	
	5.3 Tilts				
		a. x	30	‘	The tilts do not constrain the performance of the telescope up to the indicated value.
		b. y	30	‘	Obliviously, this introduces pointing errors to be modeled with T-point.

5.4 PMMA window tolerances

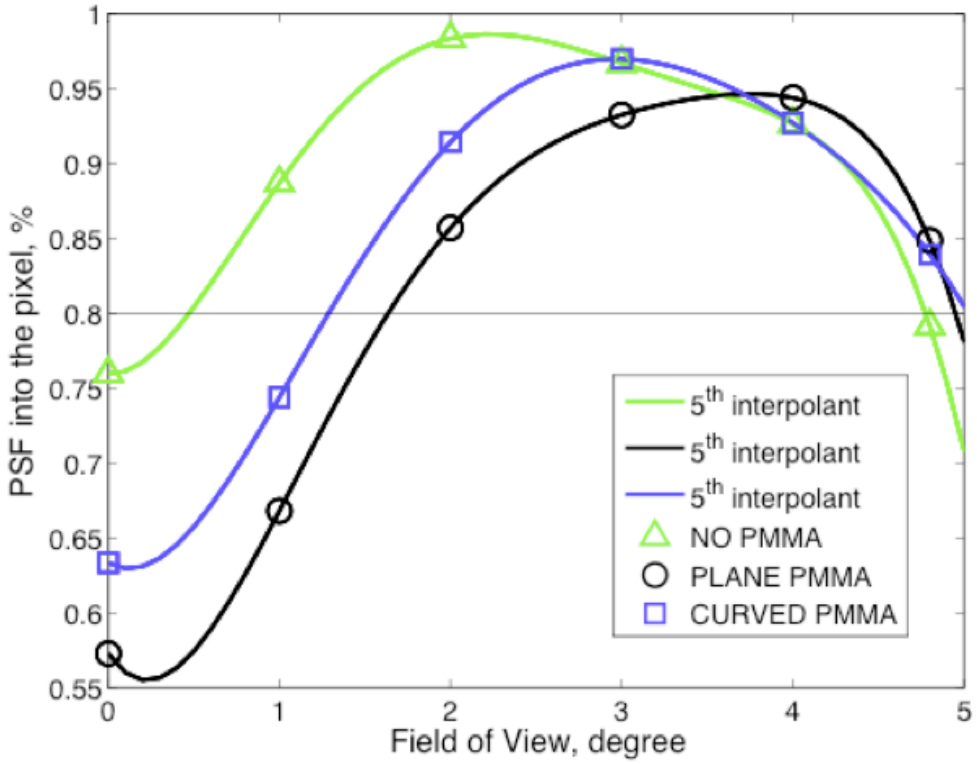
The PMMA window positioning (both plane and curved) doesn't affect significantly the properties, photometric radii and shape, of the telescope PSFs. The main modification is the change in the photons optical path that is proportional to *T/n*, with *T* thickness of the window and *n* its refraction index. The focus shift is about 3.2 mm and it could be compensated by M2 actuators. The PMMA window position is constrained by the mechanical interfaces with the LIDs; the ranges explored with the simulations are:

- 7.5 ± 2.5 mm -> plane window
- 7.75 ± 2.25 mm -> curved window

Inside this range the relative modifications on R80 is less than 3 %.

All information contained in this document is property of **INAF.** All rights reserved.

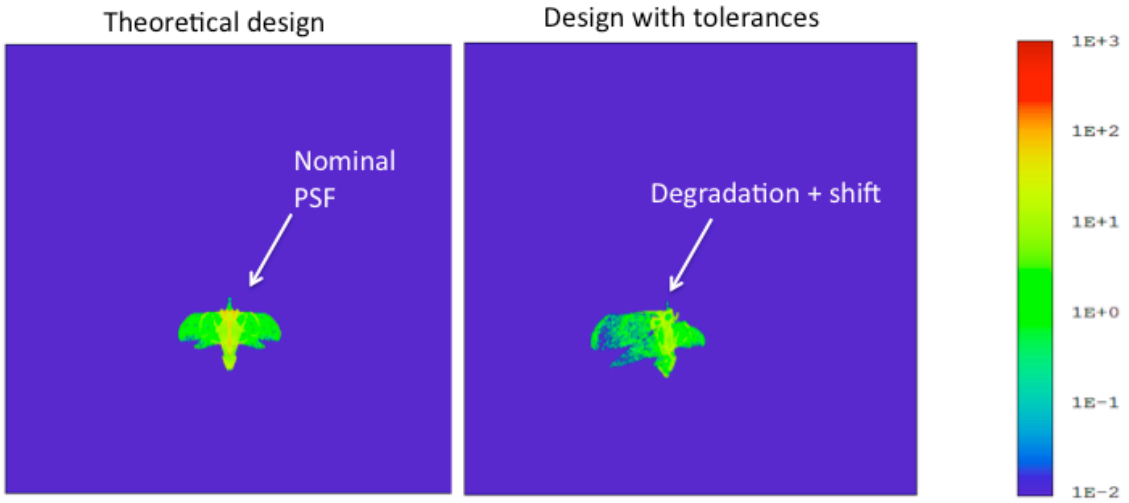
The percentage of PSF enclosed in the Cherenkov pixel for the nominal separation of the PMMA to the central PDM (7.5 mm plane, 7.75 mm curved) is plotted in figure.



All information contained in this document is property of **INAF.** All rights reserved.

6. TOLERANCE STUDY ON ERROR BUDGET

The tolerances on decentering (x,y,z) and tilts (x,y,z) for M1, M2 and camera PDMs have been put together into a series of simulations to assess the evolution of the RMS radius and centroid of the telescope PSFs. In general the tolerances on the theoretical optical design cause a degradation of the RMS radius and a change of the centroid as can be observed in the example shown in the following figure.

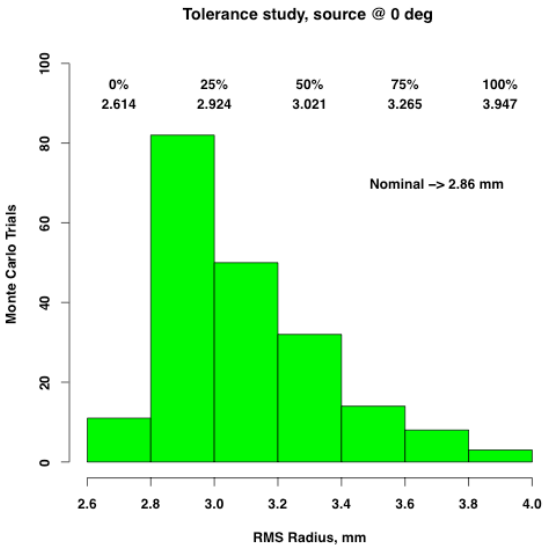


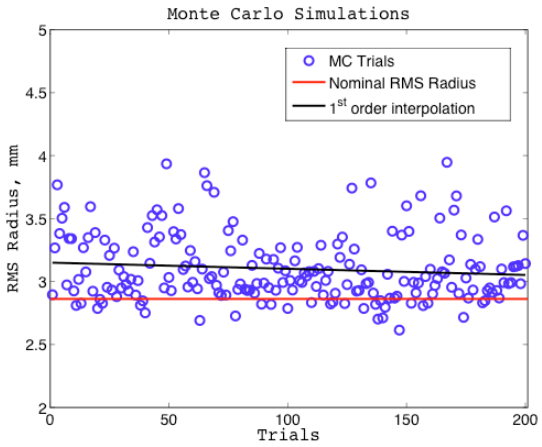
6.1 RMS Radius modifications

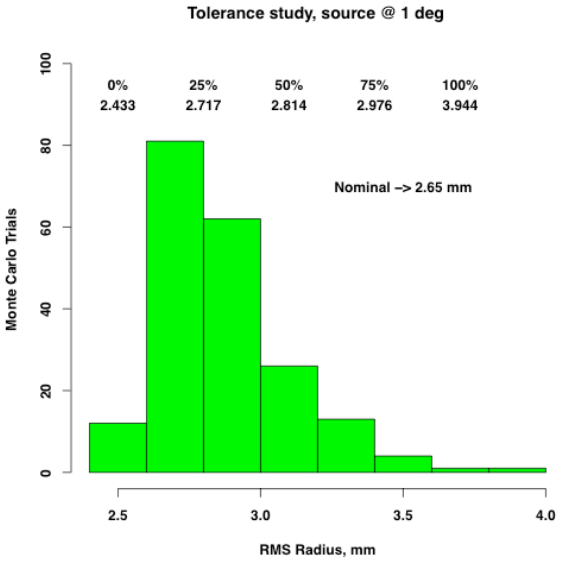
The effects of tolerances on PSF RMS radius are presented in the follow for different angles into the FoV (0°,1°,2°,3°,4°,4.8°). For each angle about 200 Monte Carlo simulations are randomly run combining the tolerances on M1, M2 and the camera PDMs; a histogram with the quartiles distribution and a scatter plot with the interpolating curve are reported to help results visualization.

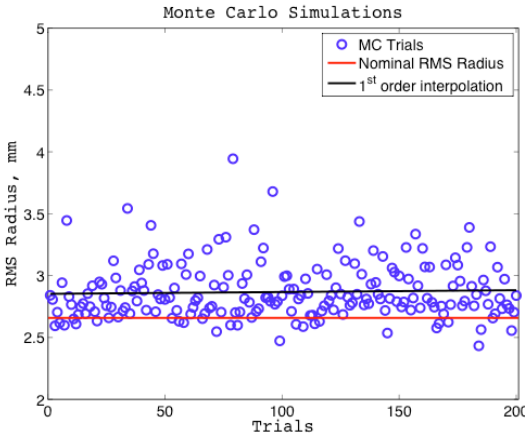
The same procedure is applied to the PSF centroid shift estimation reported in section 6.2.

All information contained in this document is property of **INAF.** All rights reserved.

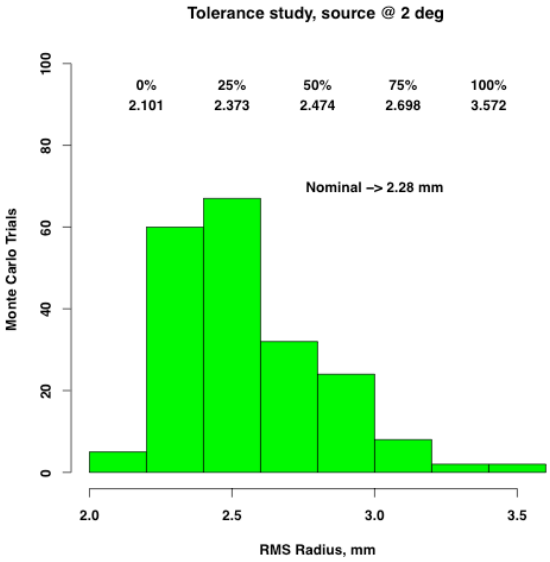


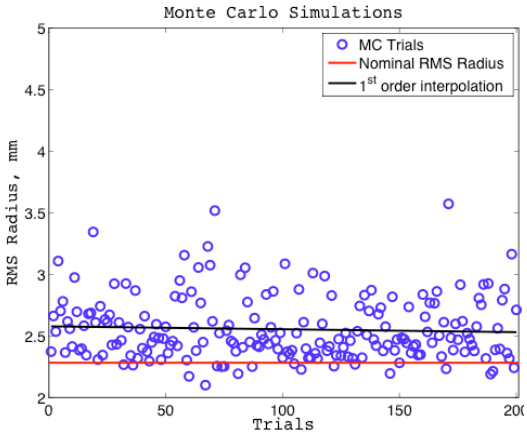


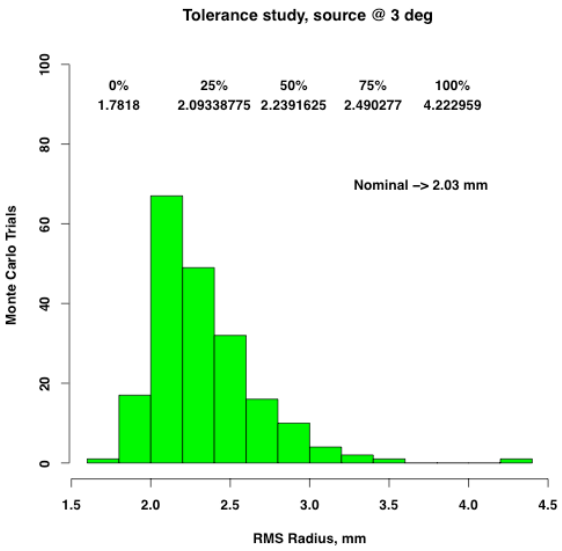


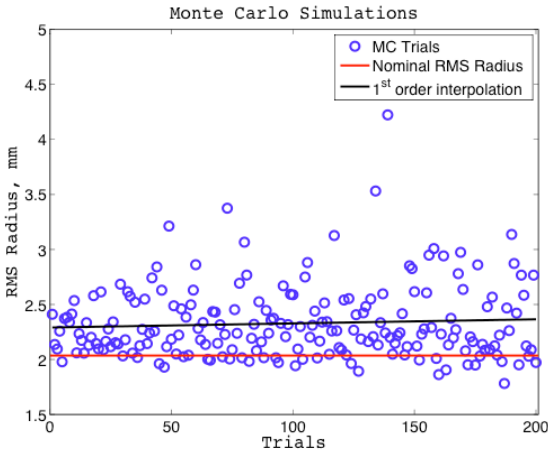


All information contained in this document is property of **INAF.** All rights reserved.

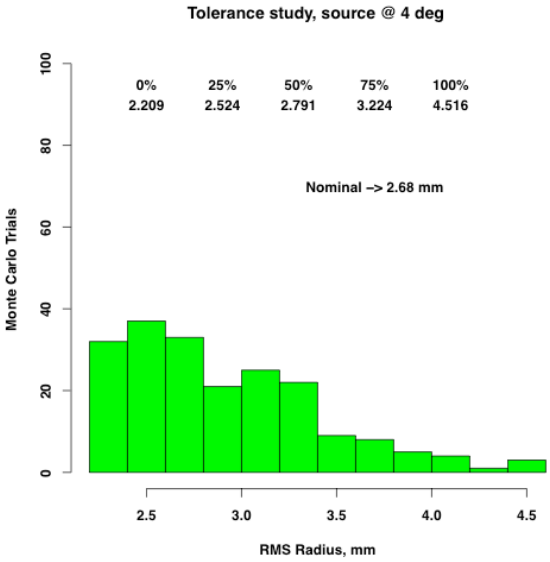


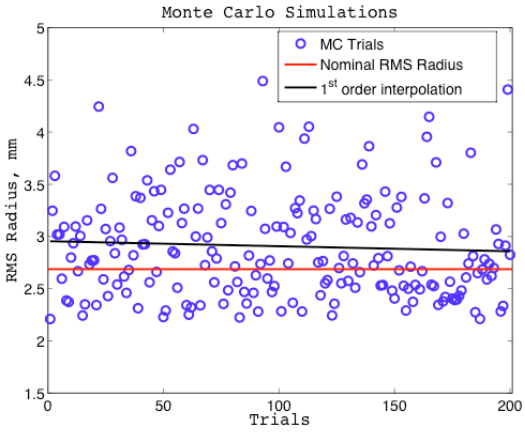


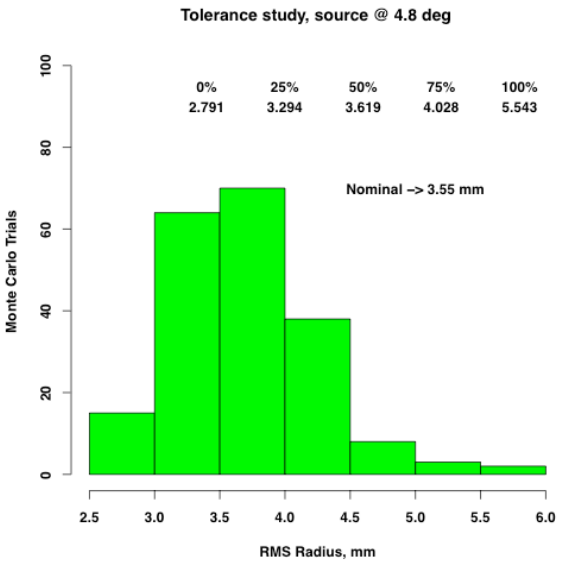


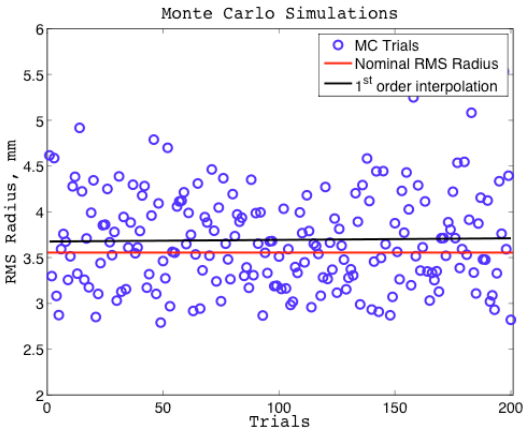


All information contained in this document is property of **INAF.** All rights reserved.



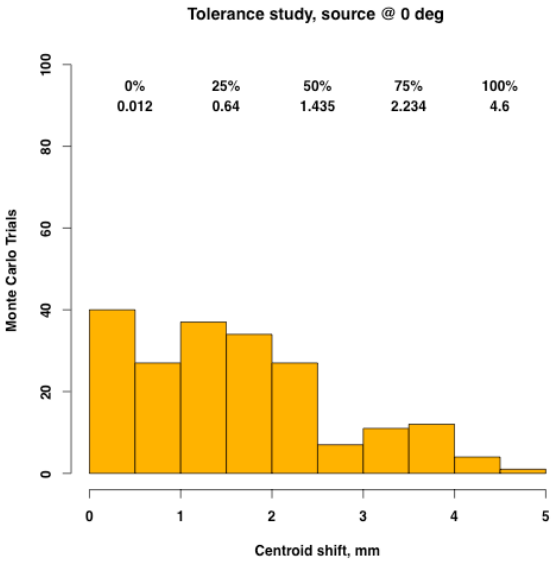


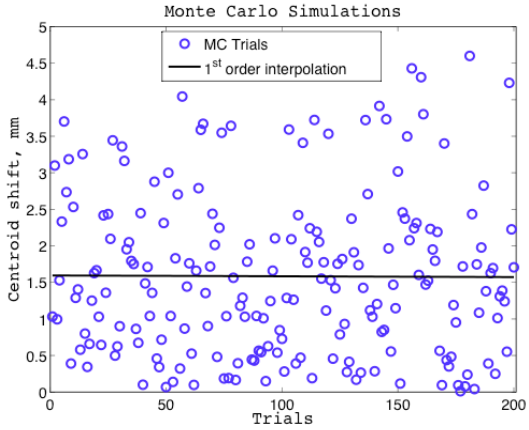


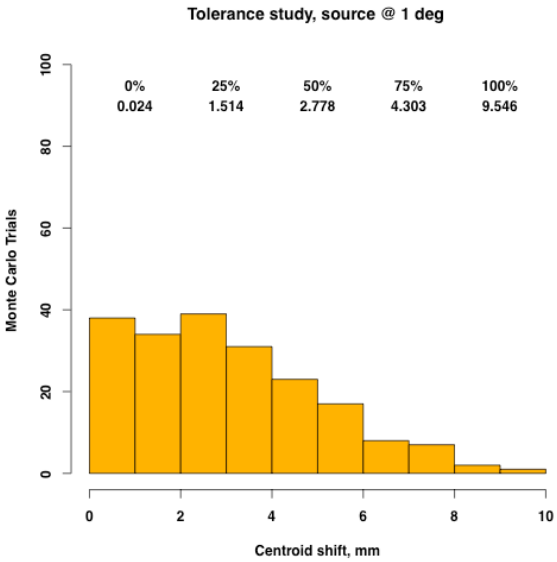


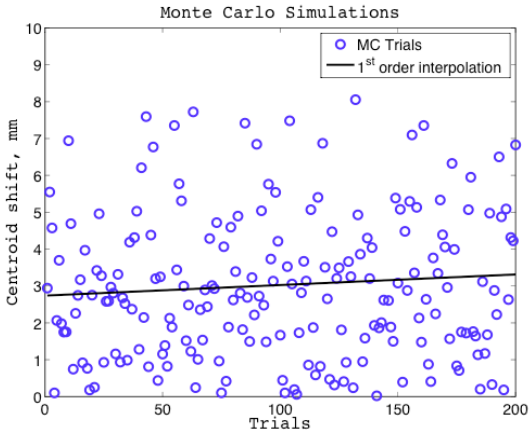
All information contained in this document is property of **INAF.** All rights reserved.

6.2 Centroid shift estimations

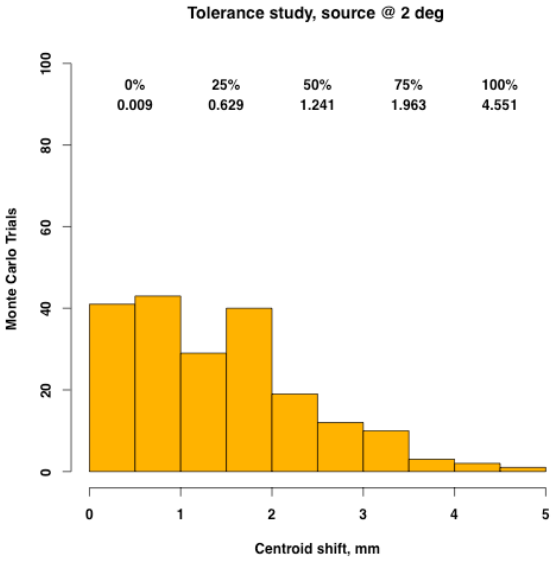


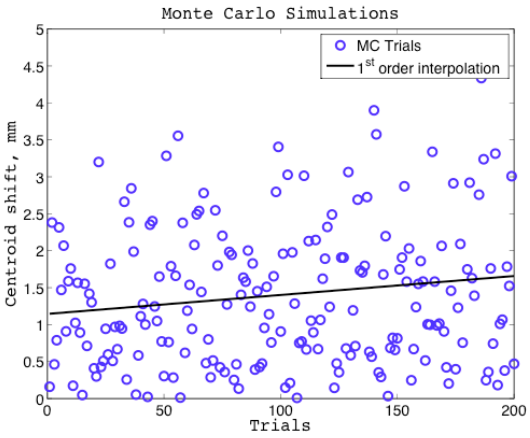


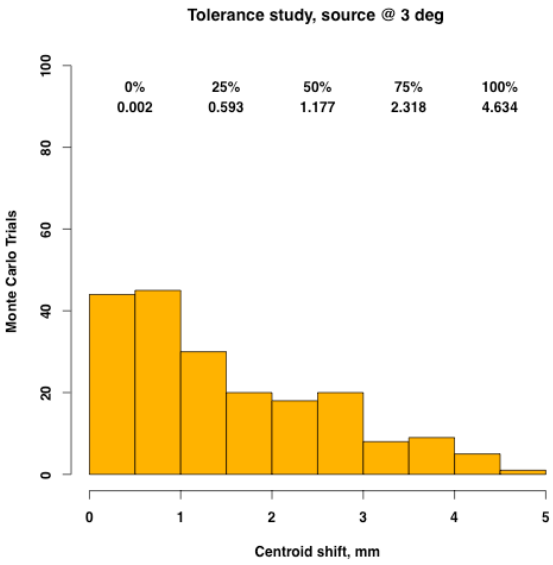


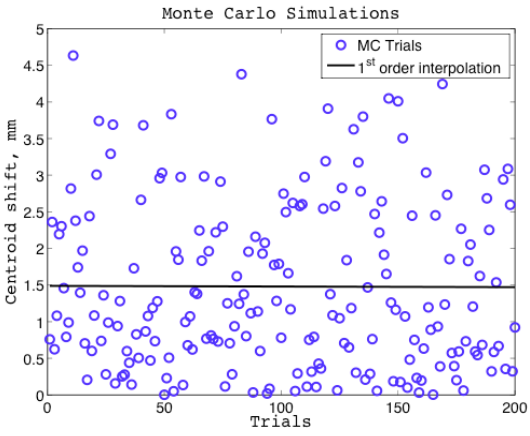


All information contained in this document is property of **INAF.** All rights reserved.

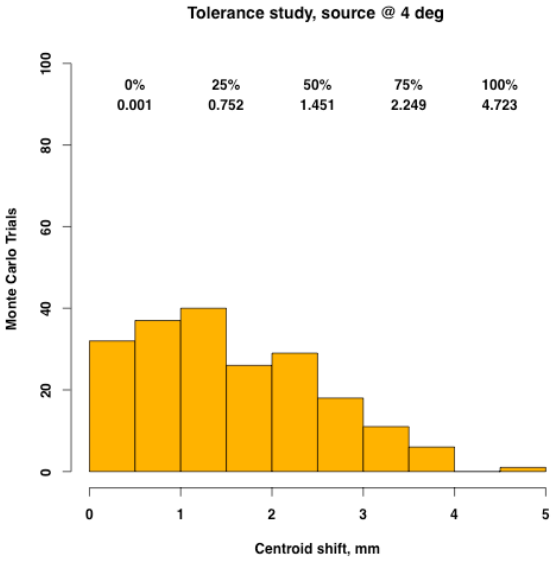


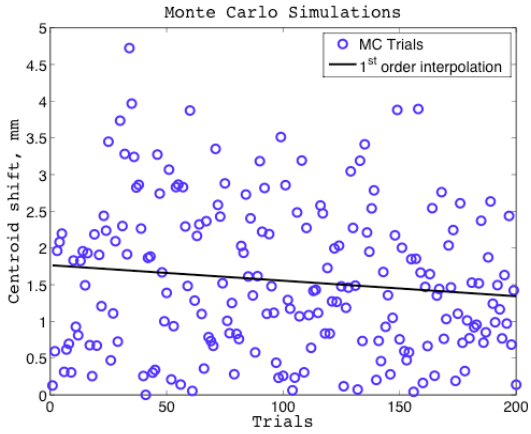


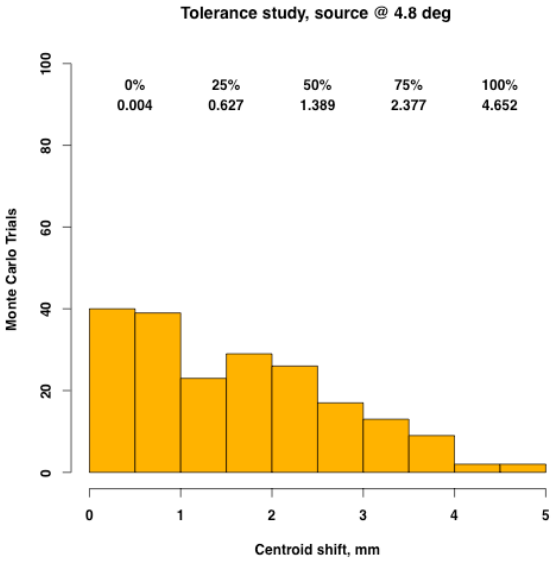


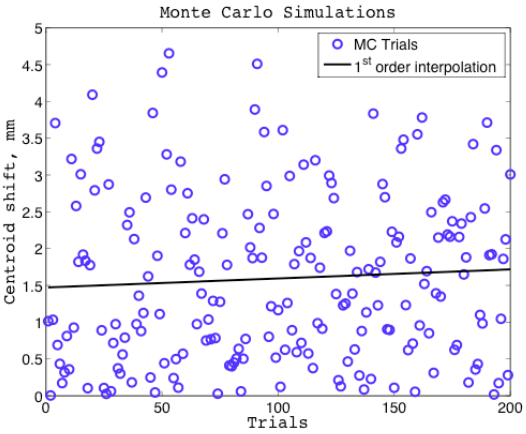


All information contained in this document is property of **INAF.** All rights reserved.









All information contained in this document is property of **INAF.** All rights reserved.